ADVANCES IN ATMOSPHERIC SCIENCES, VOL. 23, NO. 3, 2006, 449–460

Assimilated Tidal Results of Tide Gauge and TOPEX/POSEIDON Data over the China Seas Using a Variational Adjoint Approach with a Nonlinear Numerical Model

HAN Guijun*[1,2] (韩桂军), LI Wei[1,3] (李 威), HE Zhongjie[1,3] (何忠杰),
LIU Kexiu[1] (刘克修), and MA Jirui[1] (马继瑞)

[1] *National Marine Data and Information Service, State Oceanic Administration, Tianjin* 300171

[2] *International Center for Climate and Environment Science, Institute of Atmospheric Physics, Chinese Academy of Sciences, Beijing* 100029

[3] *College of Physical and Environmental Oceanography, Ocean University of China, Qingdao* 266003

(Received 5 July 2005; revised 17 November 2005)

ABSTRACT

In order to obtain an accurate tide description in the China Seas, the 2-dimensional nonlinear numerical Princeton Ocean Model (POM) is employed to incorporate *in situ* tidal measurements both from tide gauges and TOPEX/POSEIDON (T/P) derived datasets by means of the variational adjoint approach in such a way that unknown internal model parameters, bottom topography, friction coefficients and open boundary conditions, for example, are adjusted during the process. The numerical model is used as a forward model. After the along-track T/P data are processed, two classical methods, i.e. harmonic and response analysis, are implemented to estimate the tide from such datasets with a domain covering the model area extending from 0° to 41°N in latitude and from 99°E to 142°E in longitude. And the results of these two methods are compared and interpreted. The numerical simulation is performed for 16 major constituents. In the data assimilation experiments, three types of unknown parameters (water depth, bottom friction and tidal open boundary conditions in the model equations) are chosen as control variables. Among the various types of data assimilation experiments, the calibration of water depth brings the most promising results. By comparing the results with selected tide gauge data, the average absolute errors are decreased from 7.9 cm to 6.8 cm for amplitude and from 13.0° to 9.0° for phase with respect to the semidiurnal tide M_2 constituent, which is the largest tidal constituent in the model area. After the data assimilation experiment is performed, the comparison between model results and tide gauge observation for water levels shows that the RMS errors decrease by 9 cm for a total of 14 stations, mostly selected along the coast of Mainland China, when a one-month period is considered, and the correlation coefficients improve for most tidal stations among these stations.

Key words: tides, variational adjoint approach, tidal gauges, TOPEX/POSEIDON, the China Seas

doi: 10.1007/s00376-006-0449-8

1. Introduction

The hydrodynamic equations which govern the tidal elevations of the sea surface require extensive knowledge of the bottom topography underlying the continental shelf sea, in the China Seas for example. Still, for a decade, it has been more or less accepted that improved modeling of bathymetry and bottom friction by itself is insufficient to obtain more accurate solutions of the tides in such marginal seas. Also, the open boundary conditions cannot be given accurately as needed for such semi-enclosed and coastal seas. Direct observations of tidal elevations are needed to constrain the tide solutions and certain internal model parameters which may be adjusted during the process. One of the most powerful methods accomplishing such tasks is the variational adjoint approach which brings, in an extremely efficient way, the model into alignment with the observations. A good description of the method has been given by Le Dimet and Talagrand

*E-mail: gjhan@mail.nmdis.gov.cn

(1986). In the prior literature, examples for simplified geometries and synthetic observations are given. Bennett and MacIntosh (1982) published an application to a real world problem. A later work was published by Mouthaan et al. (1994), who performed an optimization using ERS-1 altimeter data to estimate the uncertain parameters in the nonlinear 2-D North Sea model, including open boundaries, bottom topography and friction coefficients. Zhu et al. (1997) discussed the optimal estimation of the open boundaries for a tidal model and gave a twin experiment. Han et al. (2000) assimilated the TOPEX/POSEIDON (T/P) derived along-track M_2 solution into the hydrodynamical model of Newfoundland. Han et al. (2001) and Han (2001) used the tide gauges and datasets from T/P to optimally control the open boundaries in the tidal model of the East China Sea. And there have been many other papers related to the issue of adjoint approach applications, for instance, Das and Lardner (1991, 1992), Lardner (1993), and Heemink and Metzelaar (1995), just to mention a few.

In this paper, the adjoint of the original model—the external mode equations of the Princeton Ocean Model (POM), namely the two-dimensional nonlinear shallow water equations, is developed, which directly yields discrete adjoint equations from finite difference discrete equations of the original model, to combine both the tide gauge data and T/P altimeter data with the model. During the optimization procedure, the uncertain parameters in the model, including both bottom topography and friction coefficients along with the open boundary conditions, are tuned to improve the simulated tide results.

The paper is organized as follows. The altimeter data processing is discussed in section 2, and two tidal analysis results are compared, namely, from harmonic analysis and response analysis. In section 3, the procedure of establishing the adjoint model of the external mode of POM is given. Data assimilation experiments combining both tide gauges and altimeter data are performed in section 4. Section 5 gives a discussion of the assimilation results and conclusions.

2. Tidal analysis

2.1 *Altimeter data processing*

The altimeter data used to compute the ocean tide, in a domain covering the model area extending from 0° to 41°N in latitude and from 99°E to 142°E in longitude, are the one-per-second altimeter measurements and corresponding corrections provided by the T/P Geophysical Data Records (GDR). The selected data are from both the TOPEX and POSEIDON altimeters and cover about ten years of the nominal mission which includes cycles 11–364. The first ten cycles were omitted because of altimeter mispointing problems (Fu et al., 1994) which resulted in poor data quality. The data processing procedure follows the steps mentioned in the paper of Liu et al. (2002). The corrected data referring to the mean sea surface are interpolated to the reference ground track in order to obtain the time series of the tidal sea surface heights at precisely the same geographical points along the track. The reference ground track is formed by searching through all the selected cycles for maximal valid observation points.

2.2 *Solution method*

Two methods have been implemented to estimate the ocean tide from along-track T/P data. The first method is the so-called response method. Munk and Cartwright (1966) represented the sea surface tidal elevation series as a limited number of constituents by assuming that the oceanic response to the tide-generating potential varies smoothly with frequency. This response method is a robust tidal analysis method which makes use of the inherent smoothness of the admittance function, whereas the traditional harmonic analysis approach (Doodson, 1921) does not. Groves and Reynolds (1975) extended the above idea by introducing a special set of orthogonal tidal functions they referred to as orthotides which overcame the weakness of non-uniques solutions to Munk and Cartwright's convolution representation. The tides in the study area are estimated by using the above method. In such an orthotide approach, the tides are expressed in the form:

$$\begin{aligned}\eta_0(t) &= \mathrm{Re}\left\{\sum_{n=2}^{3}\sum_{m=0}^{n}\sum_{k=-K}^{K}[w_{nm}(k)c^*_{nm}(t-k\Delta t)]\right\}\\ &= \sum_{n=2}^{3}\sum_{m=0}^{n}\sum_{k=-K}^{K}[u_{nm}(k)a_{nm}(t-k\Delta t)+\\ &\qquad v_{nm}(k)b_{nm}(t-k\Delta t)]\,, \end{aligned} \tag{1}$$

where a_{nm} and b_{nm} are the real and imaginary parts of the time-dependent coefficients of the tide-generating potential, i.e., $c_{nm} = a_{nm} + ib_{nm}$, and u_{nm}, v_{nm} are the corresponding weight functions particular to the location, i.e., $w_{nm} = u_{nm} + iv_{nm}$. K is a small integer and taken to be unity in practice as suggested by Cartwright (1968). The time increment Δt is chosen to be 48 h.

Equation (1) is equivalent to fitting the corresponding admittance, as follows by Fourier transforms of weight functions w:

$$\begin{aligned}Z(w) &= X(w) + iY(w)\\ &= \sum_{k=-K}^{K}[u(k)+iv(k)]\exp(-iwk\Delta t)\,, \end{aligned} \tag{2}$$

where species m and degree n are implicit.

After Groves and Reynolds (1975) replaced the non-orthogonal time functions $a_{nm}(t)$ and $b_{nm}(t)$ in Eq. (1) by a sequence of orthogonal functions derived from them, the observation equation can be written as:

$$\eta_0(t) = \sum_{m=0}^{2} \sum_{l=0}^{l_m} [U_{ml} P_{ml}(t) + V_{ml} Q_{ml}(t)] + C \,, \quad (3)$$

where n in Eq. (1) is dropped because it is limited to 2. $l_0 = 0$ and $l_1 = l_2 = 2$. $l_0 = 0$ means that we assigned a constant admittance for the long period tides in which annual ($S_{\rm a}$) and semi-annual ($S_{\rm sa}$) tides are included. U_{ml} and $V_{\rm ml}$ are the unknown parameters, related to the semidiurnal and diurnal band tides, to be solved for, and the unknown constant C in Eq. (3) is added to express the offset in η_0 due to mean sea surface error, non-tidal sea surface dynamic topography, and geographically correlated orbit error.

The explicit expressions of the orthotide functions $P_{ml}(t)$ and $Q_{\rm ml}(t)$, in terms of $a_m(t)$ and $b_m(t)$, can be found in Matsumoto et al. (1995).

The second method used in this paper to estimate the tides is the harmonic analysis approach. This method employs a least squares fit to the major tidal constituents. The ocean tide $\eta(x,t)$, at location x and time t, is generally expressed in terms of an amplitude $A_k(x)$ and Greenwich phase lag $G_k(x)$ with total N tidal components to be solved for:

$$\eta(x,t) = \sum_{k=1}^{N} A_k(x) \cos[\omega_k t + V_k - G(x)] \,, \quad (4)$$

where ω_k is the angular frequency of a tidal component. V_k is astronomical phase originating from the tide-generating potential. Argument numbers like d_1, d_2, d_3, d_4, d_5 and d_6 were introduced by Doodson (1921) to define the frequency and astronomical phase angle of each of the tidal components using the six principal astronomical arguments:

$$\begin{aligned} \omega_k t + V_k =& d_1\tau + (d_2 - 5)s + (d_3 - 5)h + \\ & (d_4 - 5)p + (d_5 - 5)N' + (d_6 - 5)p' \,, \end{aligned} \quad (5)$$

where τ, s, h, p, N', and p' are the mean lunar time, mean longitude of the moon, that of the sun, lunar perigee, lunar node, and solar perigee, respectively.

The harmonic analysis approach makes no assumptions about tidal admittances being smooth. When tidal-aliased frequencies are well separated, the solution for each constituent is largely independent of the others. Harmonic analysis also has advantages over shelf regions where shallow water tides are important due to nonlinear effects which cannot be resolved by using the response method based on a linear assumption.

The response analysis version is created to estimate 16 orthoweights and one constant at each point: 6 for each of the semidiurnal and diurnal bands and 2 for each of the long period constituents ($S_{\rm a}$ and $S_{\rm sa}$). The potential amplitudes of the constituents used are from Cartwright and Edden (1973). Twenty tidal constituents are derived directly from the orthoweights by Fourier transforms, viz., M_2, S_2, N_2, K_2, ν_2, μ_2, L_2, T_2, $2N_2$, K_1, O_1, P_1, Q_1, M_1, J_1, OO_1, ρ_1, π_1, $S_{\rm sa}$, and $S_{\rm a}$.

The harmonic analysis version is created by a least squares fit to the T/P data to estimate 24 tidal constituents in which 4 shallow water tide components are included besides the 20 constituents mentioned above, viz., Mf, Mm, M_4, and MS.

Table 1 lists the alias and Rayleigh periods for the 24 constituents which shows that the selected tides can be resolved within the T/P mission lifetime of more than 10 years because no aliasing occurs among the frequencies of these tides to be estimated.

2.3 *Comparison of harmonic and response solutions*

In this section, the response solution is compared with the harmonic solution in the region (0°–41°N, 99°–142°E) we are interested in. Obviously, the harmonic method is robust in the shallow water regions, where the nonlinear interactions of the tides with coastal topography is notable so as to result in shallow water constituents, with some having relatively large amplitudes, because it offers the advantage of being able to derive the harmonic constants of the shallow water constituents. In contrast, the response method does not. In Table 2, therefore, the results of the comparisons are given which include 8 main tidal lines, viz., M_2, S_2, N_2, K_2, K_1, O_1, P_1, and Q_1, where the regions with water depth shallower than 200 m are excluded. The root mean square (RMS) errors σ of these tidal lines are calculated according to the following equation:

$$\begin{aligned} \sigma = \Bigg\{ \frac{1}{M} \sum_{i=1}^{M} & [(H_i \cos g_i - H_i' \cos g_i')^2 + \\ & (H_i \sin g_i - H_i' \sin g_i')^2] \Bigg\}^{\frac{1}{2}} \end{aligned} \quad (6)$$

where M is the number of analysis points for comparison; and H_i and g_i (H_i' and g_i') are the amplitude and phase lag of analyzing tidal constituents from T/P altimeter data by using the harmonic method (response method).

As can be seen in Table 2, the differences between the harmonic and response solutions have an RMS on the order of less than 0.8 cm for most of the constituents. Exceptions are the K_2 and P_1 tides for which the differences are found to have an RMS of 1.5 cm or so. Hence, it may be concluded that the harmonic and response solutions are consistent to within 0.8 cm so that both methods give nearly the same results in the model area, at least for the main tidal lines.

Table 1. Tidal alias periods (on the diagonal) and Rayleigh periods (off the diagonal) in days for along-track T/P

	M_2	S_2	N_2	K_2	ν_2	μ_2	L_2	T_2	$2N_2$	K_1	O_1	P_1	Q_1	M_1	J_1	OO_1
M_2	62	1084	245	220	1303	30	31	273	35	97	173	206	594	39	69	58
S_2	–	59	316	183	592	31	32	365	37	89	206	173	384	40	74	61
N_2	–	–	50	116	206	34	35	2331	41	69	594	112	173	46	97	76
K_2	–	–	–	87	264	27	27	122	30	173	97	3353	349	33	53	46
N_2	–	–	–	–	65	30	30	226	34	105	153	245	1091	37	66	55
M_2	–	–	–	–	–	20	1303	34	206	23	37	26	29	140	53	63
L_2	–	–	–	–	–	–	21	35	245	23	38	27	29	156	56	67
T_2	–	–	–	–	–	–	–	51	41	71	473	117	187	45	93	73
$2N_2$	–	–	–	–	–	–	–	–	23	26	44	30	33	434	72	91
K_1	–	–	–	–	–	–	–	–	–	173	62	183	116	28	40	36
O_1	–	–	–	–	–	–	–	–	–	–	46	94	134	50	116	87
P_1	–	–	–	–	–	–	–	–	–	–	–	89	316	32	52	45
Q_1	–	–	–	–	–	–	–	–	–	–	–	–	69	36	62	53
M_1	–	–	–	–	–	–	–	–	–	–	–	–	–	24	87	116
J_1	–	–	–	–	–	–	–	–	–	–	–	–	–	–	33	344
OO_1	–	–	–	–	–	–	–	–	–	–	–	–	–	–	–	30
ρ_1	–	–	–	–	–	–	–	–	–	–	–	–	–	–	–	–
π_1	–	–	–	–	–	–	–	–	–	–	–	–	–	–	–	–
$S_{\rm sa}$	–	–	–	–	–	–	–	–	–	–	–	–	–	–	–	–
$S_{\rm a}$	–	–	–	–	–	–	–	–	–	–	–	–	–	–	–	–
Mf	–	–	–	–	–	–	–	–	–	–	–	–	–	–	–	–
Mm	–	–	–	–	–	–	–	–	–	–	–	–	–	–	–	–
M_4	–	–	–	–	–	–	–	–	–	–	–	–	–	–	–	–
MS	–	–	–	–	–	–	–	–	–	–	–	–	–	–	–	–

The comparison results for the tide gauge fit of the T/P solutions for four main tidal lines (M_2, S_2, K_1, O_1) are listed in Table 3. It can be seen that both methods give nearly the same results for both absolute difference values and RMS comparisons. The average absolute difference values of within 2.6 cm for amplitude and 6° for phase lag are quite acceptable.

3. Hydrodynamical model and its adjoint model

3.1 *Hydrodynamical model*

The external mode equations of the Princeton Ocean Model (POM) (Mellor, 1998), namely the two-dimensional nonlinear shallow equations, are used:

$$\frac{\partial \eta}{\partial t} + \frac{\partial UD}{\partial x} + \frac{\partial VD}{\partial y} = 0\,, \tag{7}$$

$$\frac{\partial UD}{\partial t} + \frac{\partial U^2 D}{\partial x} + \frac{\partial UVD}{\partial y} - fVD + gD\frac{\partial \eta}{\partial x} + C_{\rm b}U\sqrt{U^2+V^2} = \frac{\rho_{\rm a} C_{\rm d} W_x \sqrt{W_x^2 + W_y^2}}{\rho_{\rm w}} + \frac{\partial}{\partial x}\left(H2A_{\rm M}\frac{\partial U}{\partial x}\right) + \frac{\partial}{\partial y}\left[HA_{\rm M}\left(\frac{\partial U}{\partial y} + \frac{\partial V}{\partial x}\right)\right]\,, \tag{8}$$

$$\frac{\partial VD}{\partial t} + \frac{\partial UVD}{\partial x} + \frac{\partial V^2 D}{\partial y} + fUD + gD\frac{\partial \eta}{\partial y} + C_{\rm b}V\sqrt{U^2+V^2} = \frac{\rho_{\rm a} C_{\rm d} W_y \sqrt{W_x^2 + W_y^2}}{\rho_{\rm w}} + \frac{\partial}{\partial y}\left(H2A_{\rm M}\frac{\partial V}{\partial y}\right) + \frac{\partial}{\partial x}\left[HA_{\rm M}\left(\frac{\partial U}{\partial y} + \frac{\partial V}{\partial x}\right)\right]\,, \tag{9}$$

where x, y are the conventional cartesian coordinates, and t the time; $D \equiv H+\eta$, where $H(x,y)$ is the bottom topography and $\eta(x,y,t)$ the surface elevation; U and V are the vertically averaged velocity components; g is gravitational acceleration; f the Coriolis frequency; $C_{\rm b}$ the coefficient of bottom friction; $\rho_{\rm a}$ and $\rho_{\rm w}$ the air and sea water densities; $c_{\rm d}$ the wind drag coefficient; and $A_{\rm M}$ the horizontal eddy viscosity.

In this research, tide-generating potential is included considering that the model area of interest is large enough. The bathymetry employed in the simulations, based on ETOPO5, are built by using a horizontal resolution of 15′. The model grid spacing is

data with a repeat period of 9.9156 days.

ρ_1	π_1	$S_{\rm sa}$	$S_{\rm a}$	Mf	Mm	M_4	MS
153	473	94	75	87	50	62	66
134	329	87	70	94	52	66	62
94	161	68	57	134	62	83	52
503	410	165	114	62	40	48	94
173	743	101	79	81	48	59	69
25	28	23	22	46	77	59	21
26	29	23	22	48	82	62	21
98	173	70	59	127	60	80	53
29	33	26	24	60	124	82	23
264	122	3353	329	46	33	38	206
81	127	61	52	173	69	97	48
592	365	173	117	61	40	48	97
206	2330	112	86	76	46	56	74
31	36	27	25	69	173	101	24
48	60	40	36	349	173	594	34
42	51	36	33	173	349	819	31
105	226	245	147	55	37	44	116
–	71	117	89	73	45	55	77
–	–	183	365	45	32	37	220
–	–	–	365	40	30	34	551
–	–	–	–	36	116	220	37
–	–	–	–	–	28	245	28
–	–	–	–	–	–	31	32
–	–	–	–	–	–	–	1084

varied from 1/6° increasing to 1/2° which produces a moderate number of computational points in the model domain in order to reduce the computation time, especially during the iteration of finding an optimal solution for the adjoint approach. The bathymetry values provided by ETOPO5 in the shallow regions, such as the Pohai (Bohai) Sea for instance, are found to be highly suspect. Therefore, the bathymetry of these regions are modified by local, available nautical charts in order to obtain a more realistic coast line. The minimum depth allowed in the bathymetry is 2 m.

The finite difference scheme for the numerical discretization can be found in the users guide for the POM model of Mellor (1998).

3.2 *Adjoint model*

The cost function is defined as follows:

$$J(\boldsymbol{s}) = \frac{1}{2} w_\eta \sum_{m=1}^{M} \sum_{k=N_1}^{N} \left(\sum_{i,j} C_{i,j,m} \eta_{i,j,k} - \eta_{{\rm obs},m,k} \right)^2 + \frac{1}{2} w_s (s - s_b)^2 \,, \tag{10}$$

where $\boldsymbol{s}$ is the control parameter vector which can be chosen as coefficients of bottom friction, grid water depth, or open boundary conditions; M the total number of observation points; $[N_1, N]$ the time window for assimilation; $\eta_{\rm obs}$ the water level observation corresponding to the simulated water level value of η; w_η and w_s the weights given to the observational discrepancies and background values of control variables; and the subscripts (i, j) and superscript k denote the horizontal grid points and time step respectively.

The adjoint model is used to calculate the gradient of the cost function (10). It is developed based on a discrete numerical model, viz. the finite difference forms of Eqs. (7)–(9). The reader can refer to Han (2001) for the detailed procedure of deriving the discrete adjoint model. Note that in the experiments described in the following section, the second term in Eq. (10), which provides background information of the control variables, is ignored, because it has less importance in the adjoint data assimilation method used here compared with those background-dependent methods such as three-dimensional variational analysis (3D-VAR).

Table 2. RMS differences (cm) between harmonic and response solutions.

Tide	M_2	S_2	N_2	K_2	K_1	O_1	P_1	Q_1
cosine	0.27	0.42	0.41	1.25	0.38	0.29	0.91	0.52
sine	0.26	0.37	0.40	1.01	0.36	0.28	0.96	0.55
Total	0.37	0.56	0.57	1.60	0.53	0.40	1.32	0.75

4. Assimilation experiment

4.1 *Model setup and dataset*

Model forcing was introduced by imposing tidal elevation at the open boundaries. Here, the numerical simulation is performed for 16 major constituents including M_2, S_2, N_2, K_2, $2N_2$, μ_2, ν_2, L_2, T_2, K_1, O_1, P_1, Q_1, M_1, OO_1, and J_1. We believe that the tidal water level can be represented, within a permissible error, by making use of these constituents in the periods during which meteorological conditions have very little effect. The model is run for a period of 15 days for each constituent. After this time, the transient effects due to the initialization of the model from rest vanish.

Meteorological forcing is not taken into account in this research.

Table 3. Harmonic and response solutions fit with 20 tide gauges.

Station Name	Lat (°N)	Log (°E)	ΔH_{M2} (cm)		Δg_{M2} (°)		ΔH_{S2} (cm)	
			HAR	RES	HAR	RES	HAR	RES
SUAO	24.58	121.87	0.95	1.16	−21.12	−21.13	−0.13	0.49
OFUNTAO	39.02	141.75	2.95	2.93	0.32	0.39	1.69	1.74
NAHA	26.22	127.67	−0.01	0.62	1.75	1.89	0.96	0.16
NAZE	28.38	129.50	0.20	0.10	2.05	1.96	0.85	1.10
NISHINO	30.73	130.99	4.98	5.07	20.81	21.01	2.41	2.28
MERA	34.92	139.83	1.05	1.77	1.71	2.29	2.81	2.97
KUSHIMO	33.47	135.78	−1.86	−1.95	2.38	2.32	0.58	0.54
KUSHIRO	42.97	144.38	−0.53	−0.47	0.88	1.06	1.18	1.04
HAKODAT	41.78	140.73	−8.22	−8.21	5.80	6.52	−3.55	−4.33
ISHIGAK	24.33	124.15	−2.52	−2.77	1.01	1.01	0.55	0.39
BITUNG	1.44	125.19	2.64	2.84	5.08	5.09	−0.33	−0.34
CHENKUN	23.09	121.38	6.05	5.45	2.43	2.91	0.93	0.67
CHICHIJ	27.08	142.18	−2.07	−2.12	−2.22	−2.51	−1.32	−1.27
ABURATS	31.57	131.42	−1.00	−0.91	−0.41	−0.21	−0.27	−0.40
OFUNATO	39.07	141.72	2.93	2.91	0.27	0.34	1.69	1.74
CHICHIJI	27.10	142.18	−2.39	−2.40	−1.51	−1.72	−1.48	−1.44
GUAM	13.43	144.65	−0.24	−0.81	1.35	0.21	−0.76	0.17
SAIPAN	15.23	145.74	−1.61	−1.48	10.29	10.61	−1.73	−1.82
MALAKAL	7.33	134.46	−0.73	−0.85	12.21	12.16	−0.98	−0.65
YAP	9.52	138.13	−4.88	−4.75	2.36	2.37	−4.50	−4.11
Average			2.39	2.48	4.80	4.89	1.43	1.38
σ (cm)			7.08	7.11			2.89	2.99

Note: Phase lag is with respect to 120°E. The amplitude difference ΔH is in centimeters and the phase lag difference Δg is in degrees. HAR represents the harmonic solution and RES the response solution.

A time step is set based on the Courant-Friedrichs-Levy (CFL) computational stability condition. At $t = 0$, the initial values of $U = V = \eta = 0$ are specified at all points. The open boundary elevation for each constituent is prescribed as

$$\eta = \sum_{m=1}^{M} H_m \cos(\omega_m t - g_m) \,, \tag{11}$$

where H_m, g_m and ω_m are the amplitude, phase lag and frequency of the constituents respectively.

Note that in the experiments described below, the above formula is converted into the following format:

$$\eta = \sum_{m=1}^{M} [a_m \cos(\omega_m t) + b_m \sin(\omega_m t)] \,, \tag{12}$$

where a_m, b_m $(m = 1, \ldots, M)$ are the amplitudes of the different Fourier modes, which will be estimated as control variables illustrated in formula (10).

In the following data assimilation experiments, the harmonic constants both from the tide gauges and T/P solution in the regions with water depth deeper than 200 m are used as the observed data to calibrate the model results. Because both the harmonic and response methods give nearly the same analysis results, only the harmonic solutions are used in the assimilation procedure in the following data assimilation experiments. Figure 1 shows the location of the 83 selected tide gauge stations and ground tracks of T/P solutions in the model area. Note that not all harmonic constants are available for these tidal stations. When a harmonic constant is available, it will be brought into the model during the data assimilation procedure for the corresponding constituent. The T/P dataset is formed by choosing one T/P point with the least analysis error in each model grid corresponding to water elevation. The weight w_η in Eq. (10) for the T/P solution is assigned according to the analysis errors with a maximum value of 0.8, which enables us to obtain more realistic solutions. A similar method is also applied to the tide gauge data, but a factor of 1.0 is assigned which means that we treat these observations as 100% accurate, because published tidal constants from tide gauges are not usually accompanied by corresponding estimation errors.

$\Delta g_{S2}(^\circ)$		ΔH_{K1} (cm)		$\Delta g_{K1}(^\circ)$		ΔH_{O1} (cm)		$\Delta g_{O1}(^\circ)$	
HAR	RES	HAR	RES	HAR	RES	HAR	RES	HAR	RES
−11.82	−12.62	−0.34	−0.40	8.46	8.02	2.33	2.31	3.41	3.76
−2.56	−0.96	3.34	3.62	0.10	1.92	1.54	1.73	3.80	3.13
2.34	2.23	3.43	2.84	−3.64	−4.06	1.36	1.24	0.51	2.08
3.42	3.13	1.00	1.24	2.32	2.18	1.71	1.60	2.48	3.22
16.16	17.99	2.93	2.97	3.32	2.05	2.95	3.30	12.88	14.12
0.36	3.41	3.10	2.00	−2.77	−1.29	3.59	2.92	3.59	4.13
2.51	2.57	−0.40	−0.16	2.22	1.02	2.04	1.67	6.95	6.23
1.66	2.48	2.73	3.05	2.27	2.57	2.83	2.60	−5.41	−5.44
8.2	8.52	−8.91	−8.62	9.97	12.03	−7.01	−6.23	20.33	22.45
0.58	2.01	3.44	2.73	1.97	3.74	1.99	2.29	−0.17	0.53
6.61	5.82	5.53	5.80	0.90	1.53	2.34	2.36	−3.85	−4.66
2.84	1.54	3.00	3.08	−19.58	−20.85	0.67	0.70	−19.26	−20.5
−2.60	−4.29	0.66	0.69	−5.35	−4.76	0.71	0.41	−0.08	1.22
−5.68	−3.85	2.65	2.69	−4.65	−5.92	2.74	3.09	3.86	5.10
−2.64	−1.04	3.35	3.63	0.02	1.84	1.53	1.72	3.73	3.06
−3.56	−5.28	0.64	0.60	−4.45	−3.91	1.00	0.63	0.54	1.93
−11.33	−4.11	3.19	2.43	6.13	3.38	1.54	0.32	−1.93	−2.22
0.95	1.90	1.76	1.36	1.07	0.08	1.41	1.05	0.24	1.51
11.11	11.42	0.87	1.20	4.49	6.13	1.40	1.41	11.16	11.21
4.16	4.40	0.19	0.27	1.96	1.80	−0.15	−0.68	−1.82	−1.22
5.05	4.98	2.57	2.47	4.28	4.45	2.04	1.91	5.30	5.89
		3.73	3.69			3.19	3.15		

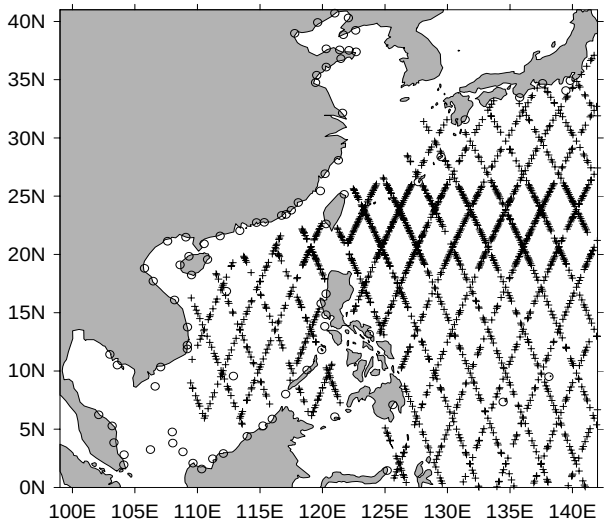

Fig. 1. Location of selected tide gauge stations (circles) and T/P ground track points (plus signs) in the China Seas.

4.2 *Data assimilation experiments and results*

4.2.1 *Harmonic constituent calibration for model simulation results*

Three types of unknown parameters, viz., water depth, bottom friction and tidal open boundary conditions, are chosen as control variables. According to different ways of combining these three types of control variables and block-set schemes (Fig. 2) for the bottom friction corrections, 11 data assimilation experiments are performed in this paper. In these experiments, water depths are corrected according to depth contours in which 10 sections are considered (Table 4). Because the given bottom topography is inaccurate in shallow waters, most sections are given in these regions. In these experiments, both tide gauge data and T/P solution data are used to calibrate these unknown parameters. Table 4 summarizes the experiment setups.

Note that the results of the experiments given here are just for the M_2 constituent. Before the data assimilation experiments are performed, the initial value of the cost function is 15040. After the data are assimilated into the model, the values of the cost function for the experiments are listed in Table 5. It should be pointed out that the model is set to 10 iterations during the optimization iteration procedure because, after 10 iterations, the assimilation result represents a satisfactory improvement over the initial guess. Also, after 10 iterations, not only is the reduction of the cost function slowed down but the assimilation results show no significant improvement but noise. The results listed in Table 5 are the best statistics for each kind of data assimilation experiment after many test

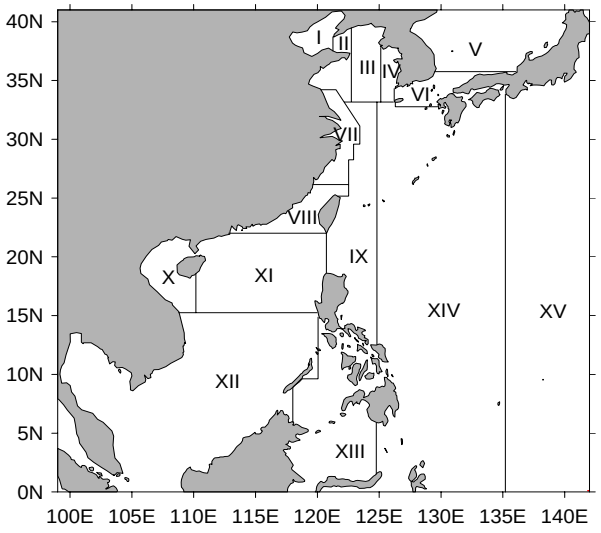

Fig. 2. Fifteen blocks are used for bottom frictions estimation in the model.

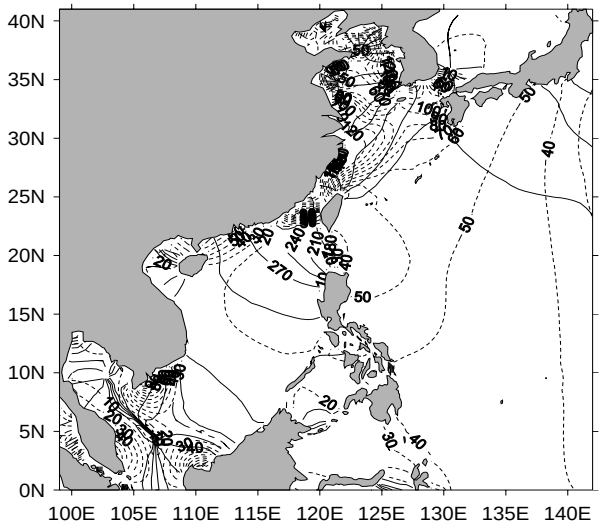

Fig. 3. Computed M_2 tidal chart using data assimilation of tide gauges and altimetric data. Dotted and solid lines denote the coamplitudes in centimeters with a 10-cm contour interval and the cophase with a 30° a contour interval, respectively. The cophase is with respect to 120°E.

cases were performed by manually adjusting the initial guesses of control parameters. It can be seen from Table 5 that the calibration of water depth brings the most promising results. Hence we adopt this kind of data assimilation scheme to perform the following discussion.

By comparing with tide gauge data in the study area, the average absolute errors of the model results are decreased from 7.9 cm to 6.8 cm for amplitude and from 13.0° to 9.0° for phase with respect to the M_2 tide.

Figure 3 presents the data assimilation results of experiment H for M_2 when T/P solutions along with the tide gauge data are assimilated into the model. In general, the coamplitudes are in agreement with the earlier studies. The semidiurnal tides in the Yellow/East China Sea display four prominent amphidromes, as can be seen in the figure. However the amphidromes in the Bay of Pohai are not as well developed in the model, probably because the topography in the Bay of Pohai is not well specified even though modified by the adjoint approach. Further effort is needed to strengthen this aspect of study by analyzing closely the nautical charts to acquire a more reasonable correction scheme for water depths. Another reason may be the fact that the model grids are not fine enough to represent such a feature in this region. The figure shows that the tides in the Yellow/East China Sea are primarily affected by the passage of the cooscillating tides from the Pacific penetrating through the Ryu Kyu Island chain. In the South China Sea, overall, our results are consistent with those from readily available literature (Fang, 1986; Fang et al., 1999). Upon comparison with the earlier studies, there is close agreement in the deep basin region of the model domain. In the coastal and gulf areas, there is more or less disagreement.

4.2.2 *Comparison between model results and tide gauge observations for water levels*

As stated above, we would compute water levels approximatively by considering 16 major constituents simulated respectively by the model when optimal estimated parameters are used. Again, the results of experiment H are used to compute the water levels at 14 tide gauge stations (station names are listed in Table 6). The time period spans about one month, from 1st March to 1st April 1996. It was found that no significant meteorological forcing occurred during this period. The values of the statistics (standard deviation and correlation coefficients) and the water levels observed and computed before and after assimilation are presented in Fig. 4 and Fig. 5 respectively. In order to show them clearly, the results for just five days (from 27th March to 1st April 1996) are given in Fig. 5.

It can be seen clearly from Fig. 4 that the performance of the model can be enhanced by correcting the water depth. The RMS error decreased by 9 cm for a total of 14 stations. For most of the stations, the RMS errors from the data assimilation experiment are smaller than those from the model simulation, and the correlation coefficients are greater. The greatest improvements, with the RMS error decreased by 42% (from 74.2 cm to 43.3 cm) and the correlation coefficient increased by 13% (from 0.84 to 0.95), are present at Lianyungang. The data assimilation model gave a little worse result at the two tidal stations of Hong Kong and Kanmen. The RMS errors increased by 1%

Table 4. Summary of experiment setups.

Experiment	Control variables	Description
B	Bottom frictions	Block set as shown in Fig. 2.
H	Water depths	10 sections are divided for water depth: <3 m, 3–5 m, 5–10 m, 10–20 m, 20–50 m, 50–100 m, 100–200 m, 200–500 m, 500–1500 m, and >1500 m. Note that in each block shown in Fig. 2 such sections are set.
OPEN	Open boundary conditions	Amplitudes of the different Fourier modes on the boundary points are estimated.
H_n	Water depths	10 sections are divided for water depth in the whole model region.
B-H	Bottom frictions and water depths	Block set as experiment B for bottom frictions, and water depths are divided as experiment H_n
B-H_n	Bottom frictions, and water depths	Block set as experiment B for bottom frictions, and water depths are divided as experiment H_n.
B-H-OPEN	Bottom frictions, water depths and open boundary conditions	Block set as experiment B for bottom frictions, and water depths are divided as experiment H_n
B-H-OPEN_n	Bottom frictions, water depths and open boundary conditions	Block set as experiment B for bottom frictions, and water depths are divided as experiment H_n.
B-OPEN	Bottom frictions and open boundary conditions	Block set as experiment B for bottom frictions.
H-OPEN	Water depths and open boundary conditions	Water depths are divided as experiment H.
H-OPEN_n	Water depths and open boundary conditions	Water depths are divided as experiment H_n.

Table 5. Values of the cost function for data assimilation experiments.

Experiment	Cost function value after assimilation	Percent improvement (%)
B	11550	23.2
H	8124	46.0
OPEN	13109	12.8
H_n	12080	19.7
B-H	9499	36.8
B-H_n	10050	33.2
B-H-OPEN	11470	23.7
B-H-OPEN_n	11470	23.7
B-OPEN	11480	23.6
H-OPEN	11940	20.6
H-OPEN_n	11850	21.2

for Hong Kong and 7% for Kanmen, and the correlation coefficients decreased by 0.3% for Hong Kong and 0.4% for Kanmen. However, it can be seen from Fig. 4 that the maximum correlation coefficient is 0.98 at Kanmen given by the data assimilation experiment. And at Hongkong, the correlation coefficient (0.80) is not the minimum. The two RMS errors are not yet the maximum. The reason for such an increase of the RMS errors may be the result of oscillation during the minimization procedure for finding the optimal solution of the adjoint approach. Such oscillation is due to the inherent errors of the observations which are not properly prescribed in the definition of the cost function.

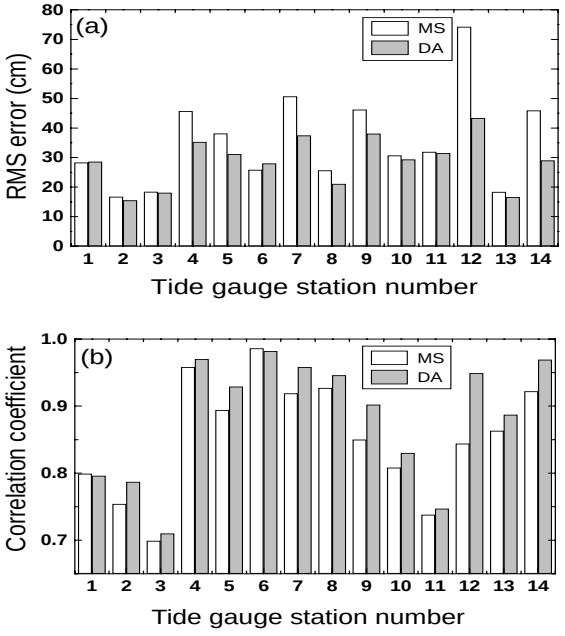

Fig. 4. (a) RMS errors and (b) correlation coefficients between observed water levels and results from model simulation and data assimilation experiments. The tide gauge station number corresponds to that in Table 6. DA indicates data assimilation results and MS the model simulations.

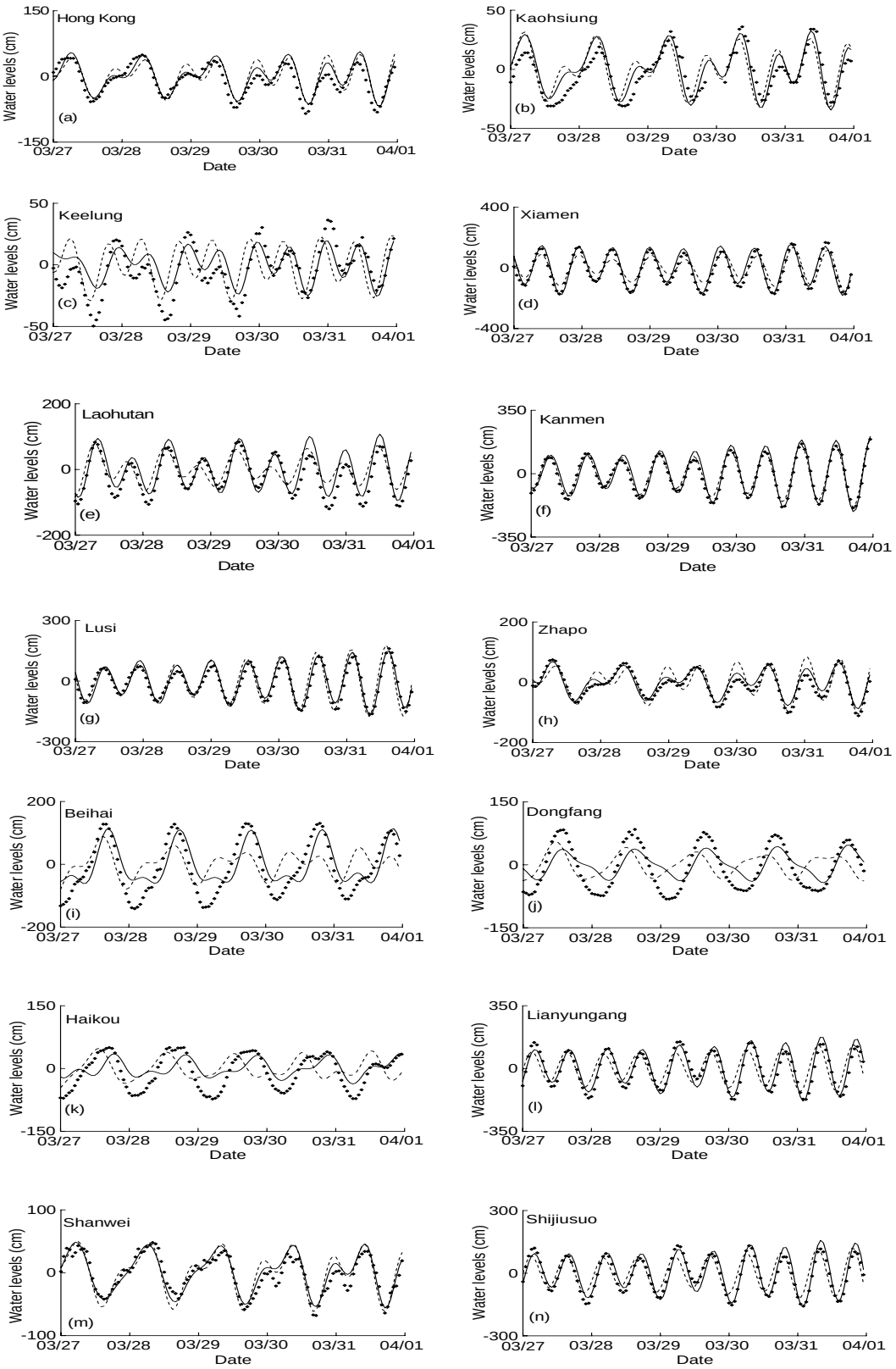

Fig. 5. Water levels from model simulations (dashed line) and data assimilation results (solid line) compared to observations (diamond) for the 5-day period (27 March–1 April 1996) for these gauge stations listed in Table 6.

Table 6. List of tide gauge stations.

No	Station name	Location		No	Station name	Location	
		Lat	Lon			Lat	Lon
1	Hong Kong	22°18′N	114°13′E	8	Zhapo	21°35′N	111°50′E
2	Kaohsiung	22°37′N	120°18′E	9	Beihai	21°29′N	109°05′E
3	Keelung	25°09′N	121°45′E	10	Dongfang	19°06′N	108°37′E
4	Xiamen	24°27′N	118°04′E	11	Haikou	20°01′N	110°17′E
5	Laohutan	38°52′N	121°41′E	12	Lianyungang	34°45′N	119°25′E
6	Kanmen	28°05′N	121°17′E	13	Shanwei	22°45′N	115°21′E
7	Lusi	32°08′N	121°37′E	14	Shijiusuo	35°23′N	119°33′E

From Fig. 5, we can see that the curves of the time series for water levels obtained from the observation and model simulation and data assimilation experiment have the same pattern as a whole, although 16 major constituents are considered in the model. Because they just show very short periods (5 days), the water levels given by the data assimilation experiment may be worse than those from the model simulations when compared with observations. For the total (approximately) one-month period, most tidal stations give promising results after the data assimilation experiment (Fig. 4).

5. Discussions and summary

In this paper, T/P altimeter data were analyzed to obtain harmonic constants of main tidal lines, and such analysis solutions along with those of tide gauges were used for calibration of a nonlinear tidal model of the China Seas which was established based on the external mode equations of the Princeton Ocean Model. In this procedure, the adjoint method was employed to establish the adjoint model corresponding to the discretized forward dynamical model. This adjoint data assimilation enhances the model's performance. Furthermore, at the same time, the model can be used to interpolate the T/P data so that the tidal movement can be reconstructed in areas for which no conventional data are available. The limitations of the adjoint modeling technique are the high storage requirements and the necessity of programming the adjoint model of the forward model. The main conclusions can be drawn as:

(1) In this study, both the harmonic and response methods gave mostly similar analysis results of T/P altimeter data with an RMS difference of 0.8 cm for most main tidal lines. And at the same time, very acceptable results were obtained by fitting them with the tide gauge data, which gave an average absolute difference of 2.6 cm for amplitude and 6° for phase lag when four main tidal lines (M_2, S_2, K_1, O_1) were considered.

(2) The adjoint model system was successfully developed and applied to calibrate depth, bottom friction and tidal open boundary conditions of the model using the T/P solution by incorporating conventional tide gauge data.

(3) After the data assimilation experiment was performed, the comparison between model results and tide gauge observation for water levels shows that the RMS errors decrease by 9 cm for a total of 14 stations when a one-month period is considered, and the correlation coefficients get better for most tidal stations among those mentioned in section 5.

Although the complex tidal dynamics in the continental shelf regions cannot be measured with altimeter data alone, these data have proved to be a valuable addition to the conventional tide gauge measurements. This is especially true in the China Seas. Much more effort is needed to further improve the above results in a follow-up study. The dual operation of T/P and JASON-1 provides an excellent opportunity. Clearly, if this effort is successful, these results will benefit people in coastal areas where accurate water level information is virtually absent.

Acknowledgments. The authors would like to thank Professor Ye Anle for his instructions on the tidal analysis of the TOPEX/POSEIDON altimeter data. Thanks go to CNES/AVISO for offering the TOPEX/POSEIDON altimeter data. This work was supported by the National Natural Science Foundation of China (Grant Nos. 40206002, 40476006, 40231014 and 40174001).

REFERENCES

Bennett, A. F., and P. C. MacIntosh, 1982: Open ocean modeling as an inverse problem: Tidal theory. *J. Phys. Oceanogr.*, **12**, 1004–1018.

Cartwright, D. E., 1968: A unified analysis of tides and surges round north and east Britain. *Philosophical Transactions of the Royal Society of London, Series A*, **263**, 1–55.

Cartwright, D. E., and A. C. Edden, 1973: Corrected tables of tidal harmonics. *Geophysical Journal of the Royal Astronomical Society.*, **33**, 253–264.

Das, S. K., and R. W. Lardner, 1991: On the estimation of parameters of hydraulic models by assimilation of periodic data. *J. Goephys. Res.*, **100**(C8), 15187–15196.

Das, S. K., and R. W. Lardner, 1992: Variational parameter estimation for a two-dimensional numerical tidal model. *International Journal for Numerical Methods in Fluids*, **15**, 313–327.

Doodson, A. T., 1921: The harmonic development of the tide-generating potential. *Proceedings of the Royal Society of London, Series A*, **100**, 305–329.

Fang Guohong, 1986: Tide and tidal current charts for the marginal seas adjacent to China. *Chinese Journal of Oceanology and Limnology*, **4**, 1–16.

Fang Guohong, Yue-Kuen Kwok, Yu Kejun, and Zhu Yaohua, 1999: Numerical simulation of principal tidal constituents in the South China Sea, Gulf of Tonkin and Gulf of Thailand. *Continental Shelf Research*, **19**, 845–869.

Fu, L. L., E. J. Christensen, C. A. Yamarone Jr., M. Lefebvre, Y. Ménard, M. Dorrer, and P. Escudier, 1994: TOPEX/POSEIDON mission overview. *J. Geophys. Res.*, **99**(C12), 24777–24797.

Groves, G. W., and R. W. Reynolds, 1975: An orthogonalized convolution method of tide prediction. *J. Geophys. Res.*, **80**(30), 4131–4138.

Han, G., R. Hendry, and M. Ikeda, 2000: Assimilating TOPEX/POSEIDON derived tides in a primitive equation model over the Newfoundland Shelf. *Continental Shelf Research*, **20**, 83–108.

Han Guijun, 2001: A study on the application of adjoint method for numerical models of tide and sea temperature. Ph. D. dissertation, Institute of Oceanology, Chinese Academy of Sciences, Qingdao, China, 110pp. (in Chinese)

Han Guijun, Fang Guohong, Ma Jirui, Liu Kexiu, and Li Dong, 2001: Optimizing open boundary conditions of nonlinear tidal model using adjoint method, ii: Assimilation experiment for tide in the Yellow Sea and East China Sea. *Acta Oceanology Sinica*, **23**(2), 25–31. (in Chinese)

Heemink, A. W., and I. D. M. Metzelaar; 1995: Data assimilation into a numerical shallow water flow model: a stochastic optimal control approach. *Jornal of Marine Systems*, **6**, 145-158.

Lardner, R. W., 1993: Optimal control of open boundary conditions for a numerical tidal model. *Computer Methods in Applied Mechanics and Engineering*, **102**, 367–387.

Le Dimet, F. X., and O. Talagrand, 1986: Variational algorithms for analysis and assimilation of meteorological observations: Theoretical aspects. *Tellus*, **38**A, 97–110.

Liu Kexiu, Ma Jirui, Han Guijun, Fan Zhenhua, and Xu Chongjin, 2002: Tidal harmonic analysis of TOPEX/POSEIDON data in Northwest Pacific by introducing difference-ratio relations. *Acta Oceanologica Sinica*, **21**(1), 33–44.

Matsumoto, K., M. Ooe, T. Sato, and J. Segawa, 1995: Ocean tide model. obtained from TOPEX/POSEIDON altimetry data. *J. Geophys. Res.*, **100**(C12), 25319-25330.

Mellor, G. L., 1998: Users guide for a three-dimensional primitive equation numerical ocean model. Program in Atmospheric and Oceanic Sciences, Princeton University, Princeton, NJ 08544-0710, 56pp.

Mouthaan, E. E. A., A. W. Heemink, and K. B. Robaczewska, 1994: Assimilation of ERS-1 altimeter data in a tidal model of the continental shelf. *Deutsche Hydrographische Zeitschrift*, **46**(4), 285–319.

Munk, W. H., and D. E. Cartwright, 1966: Tidal spectroscopy and prediction. *Phil. Trans. Roy. Soc. London, Series A*, **259**, 533–581.

Zhu Jiang, Zeng Qingchun, Guo Dongjian, and Liu Zhuo, 1997: Optimal estimation of open boundary conditions in the coastal model by using adjoint method and tide gauges data. *Science in China* (D), **27**(5), 462–468.